ISBN: 978-3-95450-231-8 ISSN: 2673-5490 doi: 10.18429/JACoW-IPAC2023-WEPL091

FAST RF TRACKING FUNCTIONS

M. Southerby[1,2*], R. Apsimon[1,2]
[1]Lancaster University, Bailrigg, Lancaster, UK
[2]Cockcroft Institute, Daresbury Laboratory, Warrington, UK

Abstract

The beam dynamics of a bunch both longitudinally and transversely play a major role in the design process of an RF cavity, from the feasibility of cavity lengths, to the focusing schemes required to maximise capture. Often, computer simulations track particles using computationally intensive numerical techniques, which can be extremely time-consuming to run. In this paper, we present a generalised analytical method to track macro-particles through RF structures, computing the 6D phase space elements at the end of each RF cell. The results show strong agreement with the well-benchmarked tracking code, ASTRA, however requires a significant reduction in computing power and run time. The results from this paper present a very promising means of streamlining future tracking simulations by increasing the computing efficiency with no significant detriment in accuracy.

INTRODUCTION

During the design process of an RF cavity for particle acceleration, the motion of a particle beam through the RF cavity must may be studied. Modern day tracking codes often utilise time-step integrators, such as RK4, alongside an imported Electromagnetic field map to determine the particle positions and momenta along the RF cavity. In this paper we outline an analytical method to determine the 6D phase space of a particle beam through an RF cavity, performing one calculation per cell length, vastly increasing the speed of particle tracking.

When a charged particle traverses an RF cell excited in the TM010 mode, the E_z field will be aligned with the z axis, and accelerate or decelerate a charged particle.

For a perfect cylindrical cell, Maxwell's equations can be solved and we find analytical exact solutions to the EM field profile, namely the Bessel functions of the first kind, $J_\alpha(x)$ [1]. The introduction of nose cones to increase the shunt impedance produces a more complex shape in which to solve Maxwell's equations. As a result EM solver codes are used to determine the field profiles. For zero radial displacement (on-axis), the fields behave the same as that of a cylindrical cell, namely both E_r and $B_\phi = 0 \; \forall$ z within the cell. Once the particles traverse the cell off-axis, E_r and B_ϕ are none zero and will effect particle motion. From Maxwell's equations, all remaining field components can be safely ignored;

$$B_z = B_r = E_\phi = 0$$

From Lorentz law, we can show the momentum change in the 3 physical dimensions in Cartesian coordinates are;

$$\mathrm{d}p_x \approx \frac{\mathrm{q}}{v_z} E_x(s,r)\mathrm{d}s - \frac{\mathrm{q}}{v_z}(v_z B_y(s,r))\mathrm{d}s \quad (1)$$

$$\mathrm{d}p_y \approx \frac{\mathrm{q}}{v_z} E_y(s,r)\mathrm{d}s + \frac{\mathrm{q}}{v_z}(v_z B_x(s,r))\mathrm{d}s \quad (2)$$

$$\mathrm{d}p_z \approx \frac{\mathrm{q}}{v_z} E_z(s,r)\mathrm{d}s \quad (3)$$

Where we have assumed $v_x, v_y << v_z$ and $\mathrm{d}t = \mathrm{d}s/v_z$ where s an on-axis longitudinal spatial variable.

By solving Maxwell's equations in cylindrical coordinates, using the symmetry of the problem and expanding in the small r limit provides a set of equations for the non zero field components. Due to the complex shape, we require information on one of the field profiles. Here we use $E_z(z, r = 0, t)$. The electromagnetic fields take the following form [2].

$$E_z(s,r,t) = \left[E_z(s,0) - \frac{r^2}{4}\left(\frac{\partial^2 E_z}{\partial z^2} + \frac{\omega^2}{c^2}E_z(s,0)\right)\right]\cos(\phi_0 + \omega t)$$

$$E_r(s,r,t) = \left[-\frac{r}{2}\frac{\partial E_z}{\partial z} + \frac{r^3}{16}\left(\frac{\partial^3 E_z}{\partial z^3} + \frac{\omega^2}{c^2}\frac{\partial E_z}{\partial z}\right)\right]\cos(\phi_0 + \omega t)$$

$$B_\phi(s,r,t) = \left[\frac{r}{2}E_z(s,0) - \frac{r^3}{16}\left(\frac{\partial^2 E_z}{\partial z^2} + \frac{\omega^2}{c^2}E_z(s,0)\right)\right]\frac{\omega}{c^2}\cos(\phi_{B,0} + \omega t)$$

Where $E_z(0,s)$ is the on-axis electric field, and $\frac{\partial^n E_z}{\partial s^n}$ is the n_{th} derivative of $E_z(0,s)$ with respect to s. ϕ_0 is the phase of the electric field components, which are $\pi/2$ out of phase with the magnetic field phase, $\phi_{B,0}$, in a cylindrical cavity.

THREE DIMENSIONAL PARTICLE TRACKING ALGORITHM

The on-axis field E_z is calculated from electromagnetic solver codes, such as CST, for a given single cell geometry. The field map can be described using a Fourier series. By assuming a pi mode structure, which repeats every 2 cells, the Fourier series can be described using only sin coefficients;

$$E_z(s, r = 0) = \sum_n^\infty b_n \sin\left(\frac{2n\pi s}{P}\right) = \sum_n^\infty b_n \sin\left(\frac{n\pi s}{L_{cell}}\right) \quad (4)$$

* m.southerby@lancaster.ac.uk

ISBN: 978-3-95450-231-8 ISSN: 2673-5490 doi: 10.18429/JACoW-IPAC2023-WEPL091

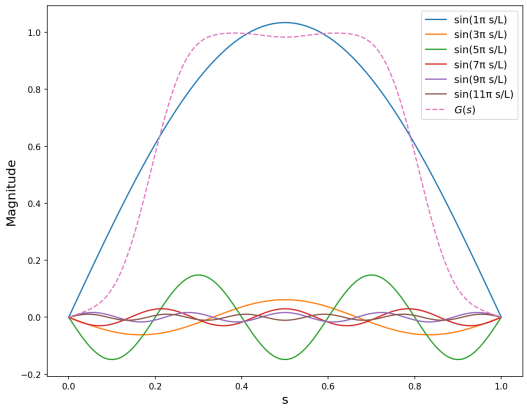

Figure 1: The on-axis E_z field described using superposition of harmonics. Actual field is shown in the dotted line.

Where the period, P = $2L_{cell}$, and $L_{cell} = \frac{\phi\beta_s c}{\omega}$ for phase advance per cell, ϕ and synchronous beta, β_s. Figure 1 shows an on axis field profile and the Fourier decomposition, only half of the period is shown.

It is simple to find the derivatives;

$$\frac{\partial E_z(r=0,s)}{\partial s} = \frac{\pi}{L}\sum_{n=0}^{\infty} b_n n \cos\left(\frac{n\pi s}{L}\right) = E_z'(s)$$

and so on for E_z'', E_z'''. We are now ready to construct the integral to find the momentum change over a distance, L, which we are free to chose. In this study we have integrated over one cell length, however there is no reason the integral can not be performed over half a cell length, or two cell lengths.

$$\mathrm{d}P_z = \frac{q}{v_z}\int_0^{L_{cell}} E_z(r,s,t)\mathrm{d}s = \frac{q}{v_z}\int_0^{L_{cell}}\left[E_z(0,s) - \frac{r^2}{4}\left(\frac{\partial^2 E_z}{\partial z^2} + \frac{\omega^2}{c^2}E_z(0,s)\right)\right] \times \cos\left(\phi_0 + \omega t\right)\mathrm{d}s$$

The temporal term that causes the electromagnetic field to oscillate at the RF frequency must be changed to the independant variable, s. We change variables using $t = \frac{s}{v_z}$ as before during the manipulation of the Lorentz force. This variable change allows us knowledge of the phase of the RF field as the particle traverses the cell. Again, this method assumes constant particle beta over the cell. Performing the integral produces the following

$$\mathrm{d}P_z = \frac{q}{v_z}\left(1 - \frac{\omega^2}{c^2}\frac{r^2}{4}\right)\frac{L_{cell}}{2\pi}F(b_{n,0},\beta_s,\beta_z,\phi_0) + \frac{q}{v_z}\frac{\pi^2}{L_{cell}}\frac{r^2}{4}\frac{1}{2\pi}F(b_{n,2},\beta_s,\beta_z,\phi_0) \quad (5)$$

Where β_z is the particle beta longitudinally, ϕ_0 is RF phase when the particle enters the cell, and

$$F(b_{n,i},\beta_s,\beta_z,\phi_0) = \sum_{n=1}^{\infty} b_n n^i \left[\frac{\cos\left(\frac{\beta_s}{\beta_z}\pi - n\pi + \phi_0\right) - \cos(\phi_0)}{\left(\frac{\beta_s}{\beta_z} - n\right)} - \frac{\cos\left(\frac{\beta_s}{\beta_z}\pi + n\pi + \phi_0\right) - \cos(\phi_0)}{\left(\frac{\beta_s}{\beta_z} + n\right)}\right]$$

Similar functional forms can be derived for the transverse phase space elements, however are not shown in this paper. A code was written in python that calculates the updated momentum and position of each particle every single cell.

$$P_{i1} = P_{i0} + \mathrm{d}P_i$$

For $i = x, y, z$. The particle position after each cell is calculated as the following;

$$X_1 = X_0 + L_{cell}\frac{\overline{\beta_X}}{\overline{\beta_z}}$$

For $X = x, y, z$. Every cell, the code must also update the new RF phase due to mismatches of the particle velocity and synchronous particle velocity leading to phase slippage.

$$\phi_{0,next} = \phi_0 + \pi\left(1 - \frac{\beta_s}{\overline{\beta_z}}\right)$$

It is now possible to analytically determine the 6D phase space change of a particle over one RF cell. Note this method does not account for space charge effects.

Traveling Wave Cavities In the above analytical interpretation, we assumed the RF cavity is excited in a standing wave mode. In order to simulate traveling wave cavities, we can treat E_z as the real component of a traveling wave with a standing wave envelope. We assume the TM010 mode is excited by an amount that is proportional to the ratio of the area of the field in a cell at any time, to the maximum area of the field in a cell, results from traveling wave tracking will not be discussed in this paper.

COMPARISON TO NUMERICAL RESULTS IN ASTRA

Figure 2 shows the transverse phase space from both ASTRA [3] and the Single Cell Fast Tracking algorithm. The same input distribution file was used, which was created using the ASTRA generator. Figure 2 shows the close agreement of the single cell function with ASTRA.

Figure 3 shows the transverse phase space plot for a 20 cell cavity for nominal proton energy 37.5 MeV. This energy level was explored as is the proton energy where RF cells excited in the TM010 mode may become utilised in proton acceleration. Lower level accelerator is often performed with RFQ and drift tube linacs. At this energy, the proton velocity increases most rapidly with energy and therefore is the range in which the single cell function is least accurate, as it assumes constant particle beta over a cell.

ISBN: 978-3-95450-231-8 ISSN: 2673-5490 doi: 10.18429/JACoW-IPAC2023-WEPL091

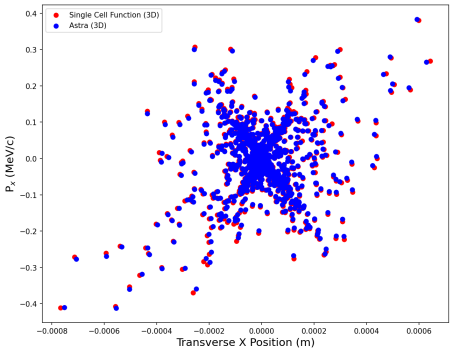

Figure 2: Transverse Phase Space plot of particle proton beam after 50 cell cavity. Particle beam input energy centered at 150 MeV.

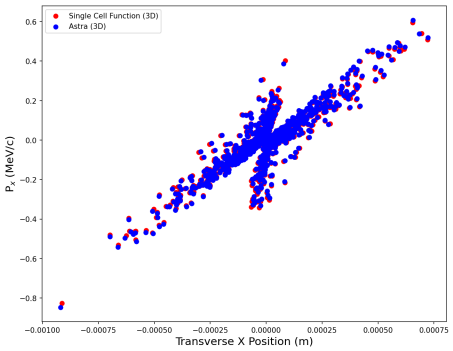

Figure 3: Transverse Phase Space plot of particle proton beam after 20 cell cavity. Particle beam input energy centered at 37.5 MeV.

Figures 4 and 5 show the longitudinal Z phase space plot for the two cavity types; 50 cell, 150 MeV and 20 cell, 37.5 MeV beams, respectively. The phase space plots show close agreement between the single cell function and ASTRA. The greatest discrepancy occurs on the neck of the separatrix or 'golf club'. This error arises as the constant beta approximation is less valid for particles between accelerating buckets.

CONCLUSION

In this paper we outline a method of fast particle tracking through an RF cavity using an analytical function to determine the momentum gain over each RF cell. The analytical functions show high accuracy with respect to well trusted tracking code, ASTRA. The method outlined was derived with respect to a TM010 cavity mode. However, there is no reason a user could not define the fields from alternative cavity modes and calculate momentum changes over a single cell.

As the single cell functions compute far fewer calculations for a given simulation, the code can be optimised and written in a compiled language to perform intense RF tracking simulations much more quickly, reducing the time taken to perform tracking simulations during accelerator design.

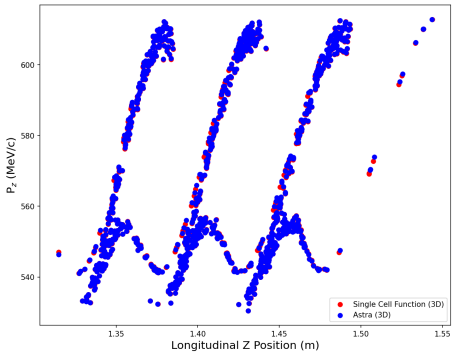

Figure 4: Longitudinal Z Phase Space plot of particle proton beam after 50 cell cavity. Particle beam input energy centered at 150 MeV.

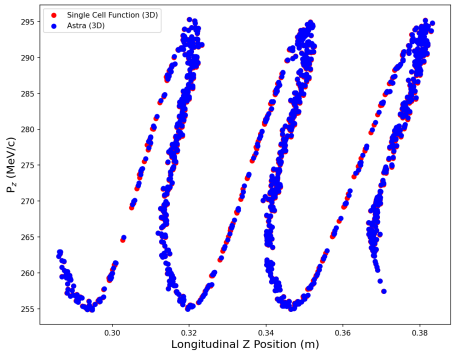

Figure 5: Longitudinal Z Phase Space plot of particle proton beam after 20 cell cavity. Particle beam input energy centered at 37.5 MeV.

REFERENCES

[1] T. Wangler, "Introduction ", in *RF Linear Accelerators*, Wiley-VCH Verlag GmbH & Co, 2008, pp. 26-28.

[2] D. Burrini, C. Pagani, and L. Serafini, "A New Analytical Model for Axi-symmetric Cavities", in *Proc. PAC'95*, Dallas, TX, USA, May 1995, paper RAQ05.

[3] K. Floettmann, "A Space Charge Tracking Algorithm", DESY, Germany, 2017.